On compact models for high-voltage MOS devices

F.P.H. van Beckum, J. Boersma, L.C.G.J.M. Habets,
G. Meinsma, J. Molenaar, W.H.A. Schilders, A.A.F. van de Ven

Abstract

Fast evaluation of integrated circuits(ICs) requires the availability of so–called *compact models*, i.e. simple–to–evaluate relations between the voltages and the currents in the IC–components. In this paper the compact model for a particular IC–part, the *LDMOS device*, is studied. This model consists of coupled submodels, each of which describes a separate part of the LDMOS device. The purpose of the present work is the derivation of the submodel for the transition region of the LDMOS. As a preparation a model for a neighbouring region, the drift region, is derived in full detail. It is shown that the submodels for transition and drift regions are very similar, although the transition region seems to be more intricate as far as its geometry is concerned. The general form of the transition region model needs evaluation of an integral. The expression can be reduced to an algebraic one if the voltages applied to the boundaries do not differ much. This insight may enhance the evaluation speed considerably.

Keywords

Transistor, Integrated circuits, High-voltage LDMOS device, Compact Model, Transition Region, Drift Region, Thin-layer Approximation, Depletion Layer

1 Introduction

An integrated circuit (IC) consists of many thousands of semiconductor devices (transistors). In practice, there is an urgent need for mathematical models of transistors, since such models allow to simulate the behavior of an IC. The physics underlying a semiconductor is reasonably well understood, so finite–element methods may be formulated that in principle may be used for simulation. Finite–element methods, however, require a lot of computing time and memory, and for a full IC with its many transistors a finite–element model per separate transistor is therefore not manageable. Instead we would like to have a compact model for a transistor with the following properties:

- the model provides a simple–to–evaluate relation between the voltages and currents at designated places in the transistor;
- the model is scalable, that is, its physical parameters and geometry may be varied such that a large class of transistors is described.

In the following section we describe the LDMOS (Lateral Double-Diffused Metal Oxide Silicon) device, used for high voltages, in some detail and specify the parameters involved. The overall model of the device will be a combination of models for various regions in the device. We identify two such regions, the *drift* region and the *transition* region. In Section 3 we review a one-dimensional depletion layer model. This is a building block for a model for

the drift region, which we consider in Section 4. Then, in Section 5 we take a closer look at the transition region, which is the region of main concern. In the process of modelling several simplifying assumptions are made along the way. The present work is not concerned with the investigation of the quality of the model developed for the transition region.

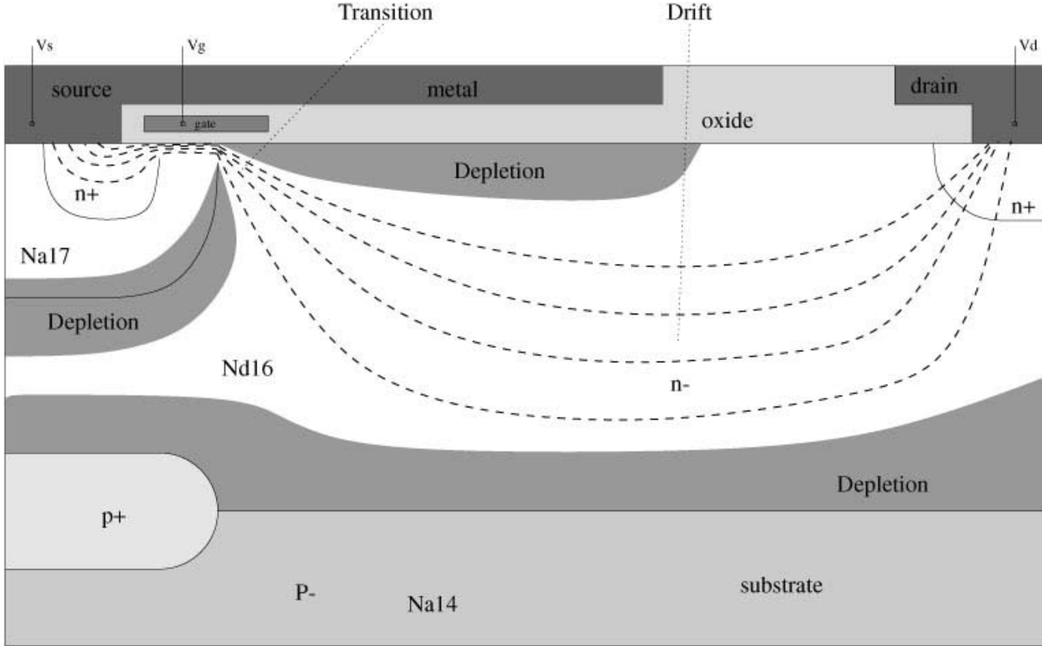

Figure 1: An LDMOS device.

2 An LDMOS device

Figure 1 shows a cross–section of an LDMOS device. In the top part a strip of oxide separates two strips of metal called the *source* (on the left) and the *drain* (on the right). If we set a voltage $V_d - V_s > 0$ across the two metal strips electrons will move from source to drain, and hence, an electric current will flow from right to left. The current lines are depicted as dashed curves in Figure 1. The current flows in the white regions which contain silicon. In fact, all material below the strip of oxide is inhomogeneous silicon, where the inhomogeneity is due to a variable amount of doping. In Figure 1 the concentrations of doping are denoted by n^- and n^+ for n–doped material (n–material), and by p^+ and p^- for p–doped material (p–material). We come back to this point in more detail in Section 3. For the moment it is enough to know that a so–called *depletion layer* is formed at places where differently doped materials meet. In Figure 1 these are the dark grey layers. They act as barriers through which only a negligible amount of current can flow. There is also a depletion layer just below the strip of oxide. The size of the depletion layers depends on the voltages, so by changing the various voltages it is possible to shrink or enlarge the depletion layers, thereby modifying the shape of the channel through which current can flow.

In the device we identify a *drift* region (a large region in the center of the device) and a tiny *transition* region (below the gate, see Figure 1). Their respective geometries differ a lot and as a result the models for them differ as well.

For the physical background of the system under consideration we refer to references [1]–[4]. Throughout we make use of the so–called drift-diffusion model, which involves the

following equations:

$$
\begin{aligned}
\mathbf{E} &= -\nabla\psi, \\
\nabla \cdot \mathbf{J} &= 0, \\
\mathbf{J} &= \underbrace{kT\mu_n \nabla n}_{\text{diffusion term}} + \underbrace{q\mu_n n\mathbf{E}}_{\text{drift term}}, \\
-\nabla(\epsilon\nabla\psi) &= \rho \;\; = q(p - n + D), \qquad (D = N_d - N_a)\ .
\end{aligned}
$$

Here, $\mathbf{E}$ is the electric field intensity, ψ is the potential, $\mathbf{J}$ is the current density, k is Boltzmann's constant, T is the temperature (in Kelvin), μ_n is the mobility of the electrons, n is the free–electron concentration, q is the electron charge, and ϵ is the permittivity of the material. The charge density, denoted by ρ, depends linearly on p, n, the concentrations of holes and free electrons, and on the doping concentration D (for a p–material $N_d = 0$, so $D = -N_a$, whereas for an n–material $N_a = 0$, and $D = N_d$. In the model it is assumed that no recombination occurs; this is expressed by the equation $\nabla \cdot \mathbf{J} = \mathbf{0}$. Some typical values and ranges of the physical quantities are listed in Table 1.

$T \approx 300$ K	$k = 1.38 \cdot 10^{-23}$ J/K	$q = 1.602 \cdot 10^{-19}$ C
$N_a = 10^{14}$ cm^{-3}	$n_i = 1.45 \cdot 10^{10}$ cm^{-3} (Silicium)	$N_d = 10^{16}$ cm^{-3}
$\mu_n = 1190$ cm^2/(Vs)	$\epsilon_{\text{ox}} = 0.345 \cdot 10^{-12}$ C/(Vcm)	$\epsilon_{\text{si}} = 1.036 \cdot 10^{-12}$ C/(Vcm)
$V_d - V_s = 12$ or 60V	$V_g - V_s = 12$ or 60V	

Table 1: Typical values and ranges of the physical quantities.

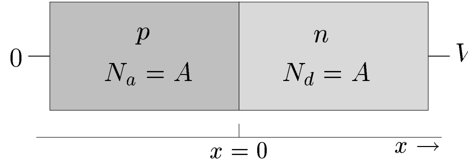

Figure 2: p-material meets n-material.

3 Depletion layers in doped material – one-dimensional case

In this section we review what happens if differently doped materials are brought in contact with each other. For simplicity we consider here the one-dimensional case of a p–material in the region $x < 0$ and an n–material in the region $x > 0$; see Figure 2. The two materials have opposite constant doping concentrations $\pm A$, so that $D = A\,\text{sgn}(x)$. We assume that a voltage difference V is applied over the two materials joined together. At the right end $(x \to \infty)$ the voltage is V, at the left end $(x \to -\infty)$ the voltage is 0. Upon contact, electrons move until after a short while a steady state is reached at which $\mathbf{J} = \mathbf{0}$. From the drift-diffusion model we then infer that

$$kT\mu_n \nabla n + q\mu_n n(-\nabla\psi) = \mathbf{0}. \tag{1}$$

In our one-dimensional configuration where $\psi(x)$ and $n(x)$ only depend on x it follows that $n(x) = c \exp\left[\frac{q}{kT}\psi(x)\right]$ for some constant c. In the steady state there is still a small percentage of the electrons that moves freely. The concentration of these electrons is denoted by n_i and for silicon $n_i = 1.45 \cdot 10^{10}\ \mathrm{cm}^{-3}$. This we can exploit for the determination of c. For large positive x the voltage $\psi(x)$ is nearly constant and close to V, hence, in the n-material we have $n(x) = n_i \exp\left[\frac{q}{kT}(\psi(x) - V)\right]$. Similarly, for large negative x the voltage $\psi(x)$ is nearly constant and close to 0. Hence in the p-material, where $q \to -q$, we have $p(x) = n_i \exp\left[-\frac{q}{kT}\psi(x)\right]$. Inserting this into the drift-diffusion model we are led to the equation

$$-\epsilon\psi''(x) = \rho(x) = qn_i\left\{\exp\left[-\frac{q}{kT}\psi(x)\right] - \exp\left[\frac{q}{kT}(\psi(x) - V)\right] + \frac{A}{n_i}\,\mathrm{sgn}(x)\right\}. \qquad (2)$$

As $x \to \pm\infty$ one has $\rho \to 0$. On neglecting exponentially small terms it follows that

$$\psi(-\infty) = -\frac{kT}{q}\log\left(\frac{A}{n_i}\right), \qquad \psi(+\infty) = V + \frac{kT}{q}\log\left(\frac{A}{n_i}\right). \qquad (3)$$

Next we multiply both sides of (2) by $\psi'(x)$ and integrate with respect to x. As a result we find

$$\begin{aligned} -\frac{1}{2}\epsilon(\psi'(x))^2 \quad &= \quad -kTn_i \exp\left[-\frac{q}{kT}\psi(x)\right] - kTn_i \exp\left[\frac{q}{kT}(\psi(x) - V)\right] \\ &\quad + qA\psi(x)\,\mathrm{sgn}(x) + C_\pm, \end{aligned} \qquad (4)$$

with integration constants C_- for $x < 0$, and C_+ for $x > 0$. These integration constants are determined by evaluating (2) at $x = \pm\infty$, where $\psi'(\pm\infty) = 0$. By use of the values of $\psi(\pm\infty)$ found above, we obtain

$$C_- = kTA\left(1 - \log\left(\frac{A}{n_i}\right)\right), \qquad C_+ = kTA\left(1 - \log\left(\frac{A}{n_i}\right)\right) - qAV. \qquad (5)$$

For reasons of symmetry we expect that $\psi(0) = V/2$. This value can be found from the property that $\psi'(x)$ is continuous at $x = 0$. Indeed, continuity of the right–hand side of (4) at $x = 0$ implies

$$-qA\psi(0) + C_- = +qA\psi(0) + C_+\ ,$$

so that $\psi(0) = (C_- - C_+)/(2qA) = V/2$. Figure 3 shows plots of the voltage $\psi(x)$, the electric field $E(x)$, and the charge density $\rho(x)$, as functions of x, for $V = 0$ and $V = 10$ and a doping concentration $A = 10^{16}\ \mathrm{cm}^{-3}$. These plots are based on a numerical solution of (4). Note the fairly abrupt transitions from a vanishing value to non–vanishing values of the charge density ρ. The *depletion layer* is now defined as the interval $[-l, l]$ outside of which $\rho(x)$ is effectively zero. The value of l may be determined by approximating $\rho(x)$ by a piecewise constant function of the form shown on the left of Figure 4. From (2) it follows that $\rho(0^-) = -qA,\ \rho(0^+) = +qA$. Corresponding approximations for ρ and E by piecewise linear and quadratic functions are obtained by integration, viz

$$E = \int_{-\infty}^{x}\frac{\rho(s)}{\epsilon}ds\ , \qquad \psi(x) = \frac{V}{2} - \int_0^x E(s)ds.$$

Plots of these approximations are shown in Figure 4. The potential $\psi(x)$ varies from $\psi(-\infty) = V/2 - qAl^2/(2\epsilon)$ till $\psi(+\infty) = V/2 + qAl^2/(2\epsilon)$. Hence by comparison with the values of $\psi(\pm\infty)$ found before, we have

$$\frac{qA}{\epsilon}l^2 = \psi(+\infty) - \psi(-\infty) = V + 2\frac{kT}{q}\log\left(\frac{A}{n_i}\right). \qquad (6)$$

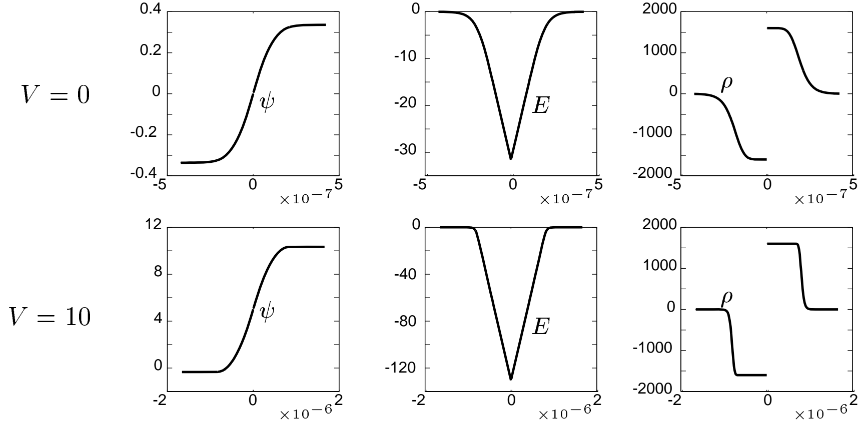

Figure 3: Plots of ψ, E and ρ across a depletion layer with $V = 0$(top) and $V = 10$ (bottom).

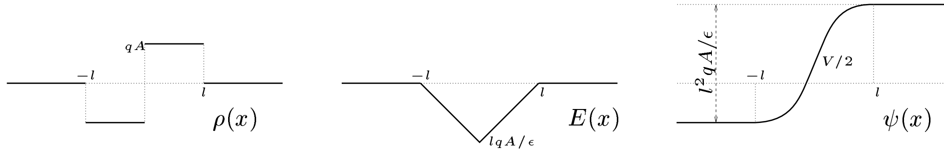

Figure 4: Figure 4: Plots of approximations of $\rho(x)$, $E(x)$, and $\psi(x)$ across a depletion layer.

This relation leads to the following expression for the width of the depletion layer as a function of the applied voltage:

$$l = \sqrt{\frac{\epsilon}{qA}(V + \psi_0)}, \qquad \psi_0 := 2\frac{kT}{q}\log\left(\frac{A}{n_i}\right). \tag{7}$$

So far we considered the case of symmetric doping: $N_d = N_a = A$. For general N_d and N_a the depletion layer is not symmetric although located around $x = 0$. It can be shown that the widths of the layers to the left and to the right of $x = 0$ are given by

$$l_a = \sqrt{\frac{\epsilon}{qN_a}\frac{2N_d}{N_a + N_d}(V + \psi_0)}, \qquad l_d = \sqrt{\frac{\epsilon}{qN_d}\frac{2N_a}{N_a + N_d}(V + \psi_0)}\ , \tag{8}$$

in which

$$\psi_0 = \frac{kT}{q}\left(\log\left(\frac{N_d}{n_i}\right) + \log\left(\frac{N_a}{n_i}\right)\right). \tag{9}$$

Finally, we consider a depletion layer from $x = 0$ till $x = l_s$, consisting of an $n-$material only. In this case, it can be shown that

$$l_s = \sqrt{\frac{2\epsilon}{qN_d}(V - V_0)}\ , \tag{10}$$

where V_0 and V are the voltages at $x = 0$ and $x \to \infty$, respectively. For the derivation of this expression we refer to the analogous derivation of the expression (32) of ϑ_s in Section 5 ((28)–(31)).

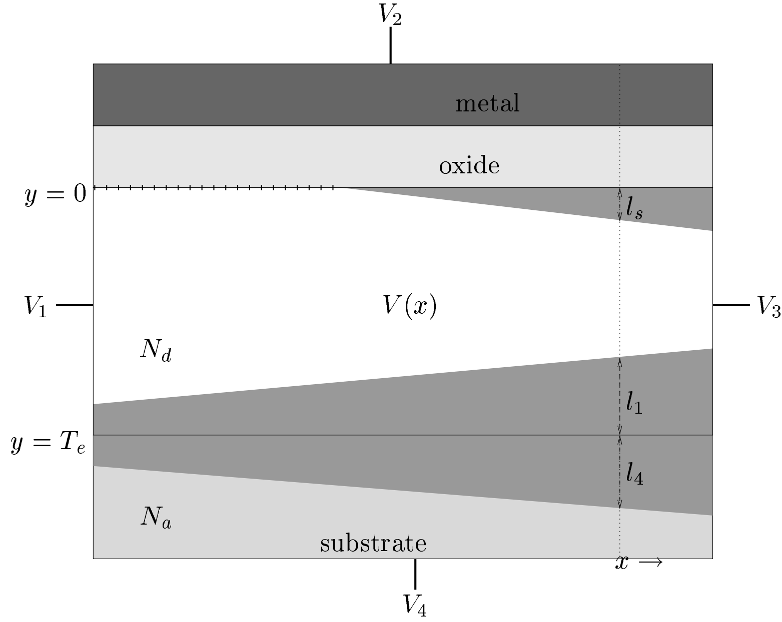

Figure 5: The drift region.

4 The drift region

With the depletion model into effect we analyze the drift region. This is the n^-–doped region G_d indicated in Figure 1 and described by $G_d := \{x, y|\, x_1 < x < x_3\ ,\ l_s(x) < y < T_e - l_1(x)\}$. In G_d the current roughly flows in the horizontal direction, from right to left, which is taken as the negative x-direction. The drift region is shown schematically in Figure 5; the four constant voltages V_i along the boundaries are assumed to be known. The aim is to relate the total current I (assumed to be constant), flowing from left to right through the drift region, to the voltages V_i. As the name suggests, in this region the effect of drift is assumed to outweigh the effect of diffusion. For the calculation of I we need the voltage $V(x, y)$ in the whole region depicted in Figure 5, so not only in G_d, but also in the metal and oxide layers and in the three depletion layers (of widths $l_s,\ l_1$ and l_4). In these different regions different asymptotics apply.
In the layers, a thin-layer-approximation may be applied, implying that the Laplace operator $\triangle V(x, y)$ in the layers reduces to

$$\triangle V \approx \frac{\partial^2 V(x,y)}{\partial y^2}\ .$$

This can be seen as follows. Let l be a characteristic length parameter for the width of the depletion layer and assume $l \ll L = x_3 - x_1$. Scale the coordinates x and y such that $x = L\hat{x},\ y = l\hat{y}$. Then the Laplace operator for V can be written in terms of $\hat{x}$ and $\hat{y}$ as

$$\triangle V = \frac{1}{L^2}\,\frac{\partial^2 V(x,y)}{\partial \hat{x}^2} + \frac{1}{l^2}\,\frac{\partial^2 V(x,y)}{\partial \hat{y}^2} = \frac{1}{l^2}\left[\left(\frac{l}{L}\right)^2\,\frac{\partial^2 V(x,y)}{\partial \hat{x}^2} + \frac{\partial^2 V(x,y)}{\partial \hat{y}^2}\right]$$

$$= \frac{1}{l^2}\frac{\partial^2 V(x,y)}{\partial \hat{y}^2}\left(1 + O((l/L)^2)\right)\ ,$$

which explains the approximation used above.
The consequence is that, for fixed x, we may now consider V as a function of y only, and

that we may use here the results of the one-dimensional models derived in Section 3.

At both sides of the interface $y = T_e$ between the n^-–doped drift region and the p^-–doped substrate a depletion layer will occur, the width of which is dependent on the voltage drop over the interface. Now suppose $V_3 > V_1 > V_4$. Then the width of the depletion layer near the right boundary $x = x_3$ (the boundary with potential V_3 in Figure 5) is larger than the width of the depletion layer near the left boundary $x = x_1$ (the boundary with potential V_1 in Figure 5). This will make the channel for the current narrowing towards the right. Under the oxide a similar depletion layer is formed, which also contributes to the reduction of the channel width towards the right. Consequently, the Ohmic resistance along the channel depends on the coordinate x.

We see that the widths of the depletion layers change, but we now assume that they change 'slowly', in so far that $|l'(x)| \ll 1$, for all $x \in (x_1,\ x_3)$. For a straight channel, the voltage in the channel will be independent of y (i.e. $V = V(x)$, then). Hence, if we assume that $|l'(x)| = O(\delta),\ 0 < \delta \ll 1$, then it is also reasonable to assume that

$$V(x,y) = V(x)(1 + O(\delta)), \qquad \text{as } (x,y) \in G_d \ .$$

Thus, for small δ, we have for the voltage in the drift region G_d:

$$V(x,y) = V(x) + \delta V_r(x,y) \ \to V(x), \qquad \text{for } \delta \ \to \ 0 \ . \tag{11}$$

The widths of the two depletion layers in the drift region, denoted by l_s and l_1, are dependent on x; see Figure 5. In fact, the widths depend on x only via the voltage V in the channel, which in its turn depends on x. Indeed, in the previous section we showed that (see (8))

$$l_1(x) = \sqrt{\frac{\epsilon_{\text{si}}}{qN_d}\frac{2N_a}{N_a + N_d}(V(x) - V_4 + \psi_0)} = \hat{l}_1(V(x)), \tag{12}$$

where

$$\psi_0 = \frac{kT}{q}\left(\log\left(\frac{N_d}{n_i}\right) + \log\left(\frac{N_a}{n_i}\right)\right) \ . \tag{13}$$

In a more or less analogous way, we can calculate $l_s(x)$. For this we start from (10). In this expression, V_0 is the voltage at $x = 0$, which is built up from the prescribed voltage V_2 and the potential jump ψ_{ox} over the oxide layer, so

$$V_0 = V_2 + \psi_{\text{ox}} \ .$$

However, ψ_{ox} also depends on l_s, as can be shown as follows.
On the interface between the metal layer (conductor) and the oxide layer (dielectric) there will be a surface charge density, say Q_2. Moreover, let the total charge per unit of length in the $x-$direction in the l_s-depletion layer be Q_s, so $Q_s = qN_d l_s$. Then, due to the global charge neutrality, we have

$$Q_2 = -Q_s = -qN_d l_s \ . \tag{14}$$

The potential jump over the oxide layer, which has width T_{ox} and permittivity ϵ_{ox}, is

$$\psi_{\text{ox}} = \frac{Q_2}{\epsilon_{\text{ox}}}\,T_{\text{ox}} = \frac{qN_d}{C_{\text{ox}}}\,l_s \ , \tag{15}$$

where

$$C_{\text{ox}} = \frac{\epsilon_{\text{ox}}}{T_{\text{ox}}} \ . \tag{16}$$

Hence,

$$V_0 = V_2 + \frac{qN_d}{C_{\text{ox}}}\ l_s\ . \tag{17}$$

Substituting this result into (10)(with $\epsilon = \epsilon_{\text{si}}$), we obtain

$$l_s^2 = \frac{2\epsilon_{\text{si}}}{qN_d}\left(V - V_2 - \frac{qN_d}{C_{\text{ox}}}\ l_s\right)\ , \tag{18}$$

resulting in the following expression for l_s:

$$l_s(x) = \sqrt{\frac{2\epsilon_{\text{si}}}{qN_d}}\left(\sqrt{V - V_2 + V_{\text{si}}} - \sqrt{V_{\text{si}}}\right) = \hat{l}_s(V)\ , \tag{19}$$

where

$$V_{\text{si}} = \frac{q\epsilon_{\text{si}}N_d}{2C_{\text{ox}}^2}\ . \tag{20}$$

Let $J(x)$ be the current density in the channel in the $x-$direction. By use of the drift-diffusion model with the diffusion term neglected, we find that the channel current density at x is given by

$$J(x) = -q\mu_n N_d \frac{dV}{dx}(x)\ . \tag{21}$$

The total current $I(x)$ flowing through a cross-section of the channel at x is then given by

$$\begin{aligned} I(x) &= W\int_{l_s(x)}^{T_e - l_1(x)} J(x)\,dy \\ &= -Wq\mu_n N_d[T_e - l_1(x) - l_s(x)]\frac{dV}{dx}(x)\ , \end{aligned} \tag{22}$$

where W is the width of the channel in the direction perpendicular to the $x-y-$plane. The relation between I and V still depends on x. However, the channel current I is independent of x, since there is no accumulation of charge. Therefore we have the obvious relation

$$I = \frac{1}{x_3 - x_1}\int_{x_1}^{x_3} I(x)dx = -\frac{W\mu_n}{x_3 - x_1}\int_{V_1}^{V_3} qN_d(T_e - \hat{l}_1(V) - \hat{l}_s(V))\,dV. \tag{23}$$

The integrand is a known function of V, hence, the total current I may be calculated as a function of V_1 and V_3: $I = I(V_1, V_3)$. To get some insight into the function $I(V_1, V_3)$, we expand it about the equilibrium point where all boundary voltages are the same: $V_1 = V_2 = V_3 = V_4$. To that end we write

$$qN_d(T_e - \hat{l}_1(V) - \hat{l}_s(V)) = \underbrace{qN_d\big(Te - \hat{l}_1(V_4)\big)}_{q_i} - \underbrace{qN_d\big(\hat{l}_1(V) - \hat{l}_1(V_4)\big)}_{q_b(V)} - \underbrace{qN_d\hat{l}_s(V)}_{q_s(V)}. \tag{24}$$

By construction, both $q_s = 0$ and $q_b = 0$ if $V_1 = V_2 = V_3 = V_4$. Therefore around the equilibrium point we have

$$\begin{aligned} I &= -\frac{W\mu_n}{x_3 - x_1}\int_{V_1}^{V_3}(q_i - q_b(V) - q_s(V))\,dV \\ &= -\frac{V_3 - V_1}{R_{\text{on}}} + \text{higher–order terms}, \end{aligned} \tag{25}$$

in which

$$R_{\text{on}} := \frac{x_3 - x_1}{W\mu_n q_i} \tag{26}$$

may be interpreted as the ohmic resistance near equilibrium.

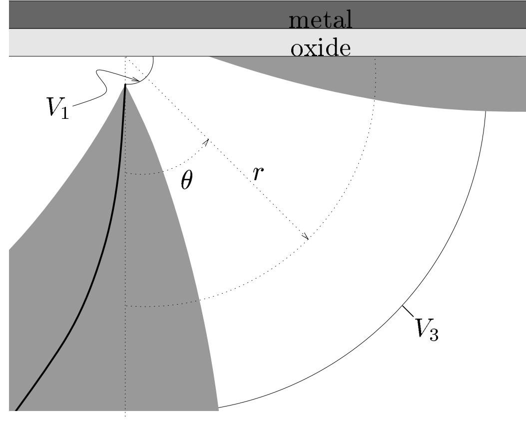

Figure 6: The transition region

5 The transition region

The transition region is a small wedge-shaped region of about $2\mu\text{m} \times 2\mu\text{m}$ below the gate, as shown in Figure 1. In the transition region we use the polar coordinates r, θ; see Figure 6. The true transition region G_t (i.e. the white region in Figure 1) is surrounded by two depletion layers, both of $n-$type. The first layer is connected to the oxide layer and runs from $\theta = 0$ to $\theta = \vartheta_s(r)$; thus the thickness of the layer at radius r is $r\vartheta_s(r)$, which should be compared to $l_s(x)$ for the drift region. The second layer runs from $\theta = \pi/2 - \vartheta_1(r)$ to $\theta = \pi/2$; here the width $r\vartheta_1(r)$ is comparable to $l_1(x)$. To the left of this layer there is a third layer, but now of $p-$type. This layer runs from $\theta = \pi/2$ to $\theta = \pi/2 + \vartheta_4(r)$ with width $r\vartheta_4(r)$ comparable to $l_4(x)$. As before, in these depletion layers $\mathbf{J} = \mathbf{0}$ and the charge density is qN_d in the ϑ_s- and ϑ_1-layers and qN_a in the ϑ_4-layer.
The true transition region is given by

$$G_t = \{r, \theta | \; r_1 < r < r_3, \; \vartheta_s(r) < \theta < \pi/2 - \vartheta_1(r)\} \; .$$

In this region a current $\mathbf{J}$ runs mainly in radial direction and dependent on r, while the charge density ρ vanishes, implying that $\triangle V = 0$. Here, $V = V(r, \theta)$ is the voltage in G_t, which has prescribed values V_1 and V_3 at the boundaries $r = r_1$ and $r = r_3$, respectively; see Figure 6.

The analysis of this wedge-shaped transition region is in main lines analogous to that of the rectangular drift region. Firstly, in the depletion layers we may apply a thin-layer-approximation, stating that we may consider the voltage at fixed r as a function of θ only, resulting in the following equation for V:

$$\frac{1}{r^2} \frac{\partial^2 V(r,\theta)}{\partial \theta^2} = -\frac{\rho}{\epsilon_{\text{si}}} \; . \tag{27}$$

In the first depletion layer this equation becomes

$$\frac{\partial^2 V_s(r,\theta)}{\partial \theta^2} = -\frac{qN_d}{\epsilon_{\text{si}}} \, r^2 \; , \qquad 0 < \theta < \vartheta_s(r) \; , \tag{28}$$

with the boundary conditions (V_2 is again the voltage applied to the oxide layer)

$$V_s(r, 0) = V_2 + \psi_{\text{ox}} \; , \qquad V_s(r, \vartheta_s) = V \; , \tag{29}$$

where

$$\psi_{\text{ox}} = \psi_{\text{ox}}(r) = \frac{qN_d}{C_{\text{ox}}}\ r\vartheta_s(r)\ , \tag{30}$$

and $V(=V(r))$ is the voltage in G_t.
The solution of this problem reads

$$V_s(r,\theta) = \frac{qN_d}{2\epsilon_{\text{si}}}\ r^2(\vartheta_s\theta - \theta^2) + V\ \frac{\theta}{\vartheta_s} + (V_2 + \psi_{\text{ox}})\left(1 - \frac{\theta}{\vartheta_s}\right)\ . \tag{31}$$

The angular width ϑ_s follows from the requirement

$$\frac{\partial V_s}{\partial \theta}(r, \vartheta_s) = 0\ ,$$

yielding

$$\vartheta_s(r) = \frac{1}{r}\sqrt{\frac{2\epsilon_{\text{si}}}{qN_d}}\left(\sqrt{V - V_2 + V_{\text{si}}} - \sqrt{V_{\text{si}}}\right) = \frac{1}{r}\ \hat{l}_s(V)\ , \tag{32}$$

with V_{si} as in (20).
It is now obvious that we can find $\vartheta_1(r)$ in accordance with (12) and (13) as

$$\vartheta_1(r) = \frac{1}{r}\sqrt{\frac{\epsilon_{\text{si}}}{qN_d}\frac{2N_a}{N_a+N_d}(V(r) - V_4 + \psi_0)} = \frac{1}{r}\ \hat{l}_1(V), \tag{33}$$

Secondly, in the transition region G_t we assume that the voltage is independent of θ, so that $V = V(r)$. This assumption can be justified as follows. Since $\rho = 0$ in G_t, V satisfies $\triangle V = 0$, and then it follows from a separation–of–variables argument that V is of the form

$$V(r,\theta) = a_0 + a_1 \log(r) + \sum_{n\in\mathbb{Z}} r^n(c_n\cos(n\theta) + d_n\sin(n\theta)). \tag{34}$$

If the boundaries of the depletion layers would be perfectly straight (i.e. $\vartheta_s(r) = \vartheta_s$ and $\vartheta_1(r) = \vartheta_1$), the boundary conditions for V would read: $V(r_1,\theta) = V_1$; $V(r_3,\theta) = V_3$; $\partial V/\partial\theta = 0$ for $\theta = \vartheta_s$ and $\theta = \vartheta_1$. This would imply that $c_n = d_n = 0$, for all n, so $V = V(r)$. Hence, when we assume that the boundaries of the depletion layers are 'slowly varying', it is allowed (in accordance with the approach for the drift region; compare to (11)) to take

$$V(r,\theta) = V(r) + \delta V_r(r,\theta)\ .$$

Thus, with $V(r_1) = V_1$ and $V(r_3) = V_3$ we obtain (up to $O(\delta)$)

$$V(r) = V_1 + \frac{V_3 - V_1}{\log(r_3/r_1)}\log\left(\frac{r}{r_1}\right). \tag{35}$$

Similar to (21) and (22), the current density and the total current through the channel in the transition region are now given by ($\mathbf{J} = J(r)\mathbf{e}_r$)

$$J(r) = -q\mu_n N_d\ \frac{dV(r)}{dr}\ , \tag{36}$$

and

$$
\begin{aligned}
I(r) &= W \int_{\vartheta_s(r)}^{\frac{\pi}{2}-\vartheta_1(r)} J(r)\, r d\theta \\
&= -Wq\mu_n N_d \left[\frac{\pi}{2} - \vartheta_1(r) - \vartheta_s(r)\right] r \frac{dV(r)}{dr} \\
&= -Wq\mu_n N_d \left[\frac{\pi}{2} r \frac{dV(r)}{dr} - \hat{l}_1(V_4)\frac{dV(r)}{dr}\right] \\
&\quad +Wq\mu_n N_d \left[\hat{l}_1(V) - \hat{l}_1(V_4)\right] \frac{dV(r)}{dr} \\
&\quad +Wq\mu_n N_d \left[\hat{l}_s(V)\frac{dV(r)}{dr}\right] \\
&= -W\mu_n \left[q_i(r) - (q_b(V) + q_s(V))\frac{dV}{dr}\right] \ , \qquad (37)
\end{aligned}
$$

where q_b and q_s are defined in (24), and q_i is given by

$$
q_i(r) = qN_d \left[\frac{\pi}{2} r - \hat{l}_1(V_4)\right] \frac{dV(r)}{dr} \ , \qquad (38)
$$

while it follows from (33) that

$$
\hat{l}_1(V_4) = \sqrt{\frac{\epsilon_{\rm si}}{qN_d}\frac{2N_a}{N_a+N_d}\psi_0} \ . \qquad (39)
$$

Since there is no accumulation of charge we again argue that

$$
\begin{aligned}
I &= \frac{1}{r_3 - r_1}\int_{r_1}^{r_3} I(r)\, dr \\
&= -\frac{W\mu_n}{r_3 - r_1}\ \frac{qN_d(V_3 - V_1)}{\log(r_3/r_1)}\ \int_{r_1}^{r_3} \left(\frac{\pi}{2} - \frac{\hat{l}_1(V_4)}{r}\right) dr \\
&\quad -\frac{W\mu_n}{r_3 - r_1}\int_{V_1}^{V_3} (q_b(V) + q_s(V))\, dV \ . \qquad (40)
\end{aligned}
$$

Around the equilibrium point $V_1 = V_2 = V_3 = V_4$, where $q_b = q_s = 0$, the total current is given by

$$
\begin{aligned}
I &= -\frac{\pi}{2}\ \frac{\mu_n q N_d W}{\log(r_3/r_1)} \left[1 - \frac{2}{\pi}\hat{l}_1(V_4)\frac{\log(r_3/r_1)}{r_3 - r_1}\right](V_3 - V_1) + \text{higher–order terms} \\
&= -\frac{V_3 - V_1}{\hat{R}_{\rm on}} + \text{higher–order terms} \ , \qquad (41)
\end{aligned}
$$

in which the ohmic resistance is given by

$$
\frac{1}{\hat{R}_o n} = \frac{\pi}{2}\ \frac{\mu_n q N_d W}{\log(r_3/r_1)} \left[1 - \frac{2}{\pi}\hat{l}_1(V_4)\frac{\log(r_3/r_1)}{r_3 - r_1}\right] . \qquad (42)
$$

With this final result, the total current in the transition region is written in a form similar to the one obtained in the drift region.

According to the numerical values of Table 1, and with $r_3 = 2\mu$m, the second term between the square brackets on the right-hand side of (41) is of the order of 10^{-1}. Hence, it is less than 1, but not really negligible with respect to 1.

6 Concluding remarks

A high–voltage MOS(metal–oxide–silicon) device consists of several regions, such as the body region, the drift region, and the transition region. A compact model for the device as a whole requires coupling of the compact models for these separate regions. Up to now, one uses for the transition region a model that has been developed for the drift region and is adapted to the transition region via ad-hoc considerations. The main goal of the present project is the derivation of a reliable compact model for the transition region from first principles. Since the drift and transition regions have the same characteristics and differ mainly in geometry, it is to be expected that many similarities exist between the corresponding models. That is why the Study-group started with rederiving the drift region model in full detail, in order to find which mechanisms are most important. For this, the basic principles described in [1]–[4] formed the starting points.

An important ingredient of a compact model for the drift region is the thin-layer-approximation for the depletion layers. Another assumption is that the widths of these layers vary rather slowly in the longitudinal direction of the channel. This implies that, to lowest order, the voltage in the drift region is a function of the horizontal position only. This approach resulted in the compact model embodied in expression (23), which relates the current through the channel to the voltages applied at the boundaries. This model contains an integral. If the boundary voltages are nearly equal, the model is described by expression (25), which is algebraic and extremely simple to evaluate.

The derivation of the drift region model provided the insights for the derivation of the transition region model. Here, polar coordinates (r, θ) are used. It is shown that the voltage in the transition region is a function of r only, if the form of the depletion layers is wedge-like with straight boundaries, i.e. $\theta =$ constant along these boundaries. It is assumed that the deviations from straight lines are small, so that, to lowest order, the θ–dependence of the voltage may be ignored. This allows for a derivation along the same lines as followed for the drift region. The resulting compact model given in (40), relates the current through the transition region to the voltages applied to the boundaries of this region. If the latter voltages are nearly equal, the model is described by (41). The latter algebraic expression, which is very easy to evaluate, shows that, to lowest order, the current is given by Ohm's law: it is proportional to the voltage difference $V_3 - V_1$ over the transition channel, and the resistance, given by (42), is a function of geometry and the other boundary voltages.

We conclude that both the drift and the transition regions of the MOS-device can be adequately represented by compact models and these models are quite similar. The models, derived above, are reliable as long as in the drift region the depletion layers vary slowly in width, whereas in the transition region the boundaries of the depletion layers do not strongly deviate from straight lines. If these conditions are not fulfilled, the present models could be extended with correction terms.

References

1. Klaassen, F.M., *Compact models for circuit simulation*, Springer, Vienna, 1989.

2. Muller, R.S. and Kamins, T.I., *Device electronics for integrated circuits*, John Wiley & Sons, New York, 1986.

3. Sze, S.M., *Physics of semiconductor devices*, John Wiley & Sons, New York, 1981.

4. Tsividis, Y., *Operation and modeling of the MOS-transistor*, Mac Graw-Hill, Boston, 1999.